Int J Adv Manuf Technol (2013) 69:2723–2733
DOI 10.1007/s00170-013-5242-0

ORIGINAL ARTICLE

Two-dimensional vibration-assisted magnetic abrasive finishing of stainless steel SUS304

Yi-Hsun Lee · Kun-Ling Wu · Jhan-Huang Jhou · Yung-Hsing Tsai · Biing-Hwa Yan

Received: 27 February 2013 / Accepted: 29 July 2013 / Published online: 16 August 2013

Abstract Traditional magnetic abrasive finishing (MAF) involves unidirectional polishing of surface but suffers the drawback of forming deep scratches, resulting in poor surface quality. This study attempts to enhance the polishing efficiency of MAF by adding vibration to the platform, focusing on the fabrication of the two-dimensional vibration-assisted MAF (2D VAMAF) setup. Experiments are conducted with variations in parameter levels of 2D VAMAF. Comparison of finished surface results shows superiority of 2D VAMAF in obtaining lower surface roughness and mirror surface quality. In addition, this study uses the Taguchi experimental design method to obtain the optimal parameter combination of 2D VAMAF for surface roughness improvement. The optimal combination obtained includes working gap (1 mm) and weight of SiC, steel particles, and machining fluid (1 g, 1.5 g and 3 g, respectively); frequency of vibration along X and Y directions (16.67 Hz); rotational speed of magnet (500 rpm); and size of SiC and steel particles (8000 and #120, respectively). With 5-min 2D VAMAF under optimal parameter combination, the surface roughness of a stainless steel SUS304 workpiece can be reduced from 0.13 to 0.03 μm, an improvement of 77 %. Experimental results reveal that 2D VAMAF can indeed improve surface quality with a shorter processing time and a smaller amount of abrasives required, both of which contribute to cost reduction. With less pollution incurred, 2D VAMAF is a more environmental friendly machining method in industry.

Keywords Two-dimensional vibration-assisted MAF (2D VAMAF) · Magnetic abrasive finishing (MAF) · Vibration assistance · Stainless steel · Surface roughness · SiC abrasives

1 Introduction

Current machining techniques have to satisfy the need for high quality and high efficiency while at the same time being environmental friendly. In terms of such requirements, magnetic abrasive finishing (MAF) is an ideal machining approach. MAF involves unidirectional polishing of surface, during which the gap between the workpiece and the magnet is filled with ferromagnetic particles and the grinding pressure is controlled by a magnetic field. Under the magnetic field, the abrasives will gather to form a flexible magnetic brush which does not require dressing. Thus, the magnetic abrasives can move and polish along the profile of a complex surface. MAF can be applied to polishing flat, curved, or uneven surface [1–5]; as well as nonconductive and nonmagnetic materials such as ceramics, plastic, glass, copper, and aluminum. While MAF is versatile in application, it suffers the drawback of forming deep scratches, resulting in poor surface quality. In view of such, this study explores adding vibration to MAF for surface roughness improvement.

There have been studies on MAF with and without vibration assistance and its applications. To name a few, Mulik and Pandey [6, 7] integrated ultrasonic vibrations with MAF to process AISI 52100 steel surfaces. Yin and Shinmura [8] applied

Y.-H. Lee · J.-H. Jhou · Y.-H. Tsai · B.-H. Yan
Department of Mechanical Engineering, National Central University, Chung-Li, Taiwan, Republic of China

K.-L. Wu
Department of Mechanical Engineering, Tungnan University, New Taipei City, Taiwan, Republic of China

B.-H. Yan (✉)
Department of Mechanical Engineering, National Central University, No.300, Jhongda Rd., Jhongli City, Taoyuan County 32001, Taiwan, Republic of China
e-mail: bhyen@cc.ncu.edu.tw

vertical vibration-assisted MAF to deburring magnesium alloy and obtained more efficient material removal compared with deburring of brass and stainless steel. Wang and Hu [9] explored the impact of various key MAF parameters including supply, material and manufacturing of magnetic abrasive, polishing speed, and grain size. Wang et al. [10] examined the finishing characteristics of Si_3N_4 fine ceramic tubes processed by magnetic field-assisted mechanochemical polishing using Cr_2O_3 abrasive mixed with magnetic particles. It was found that more efficient polishing and better surface quality can be obtained by wet finishing using distilled water than dry finishing. Jain et al. [1] studied the effect of working gap and circumferential speed on the material removal rate (MRR) and surface roughness. Their findings reveal that the larger the

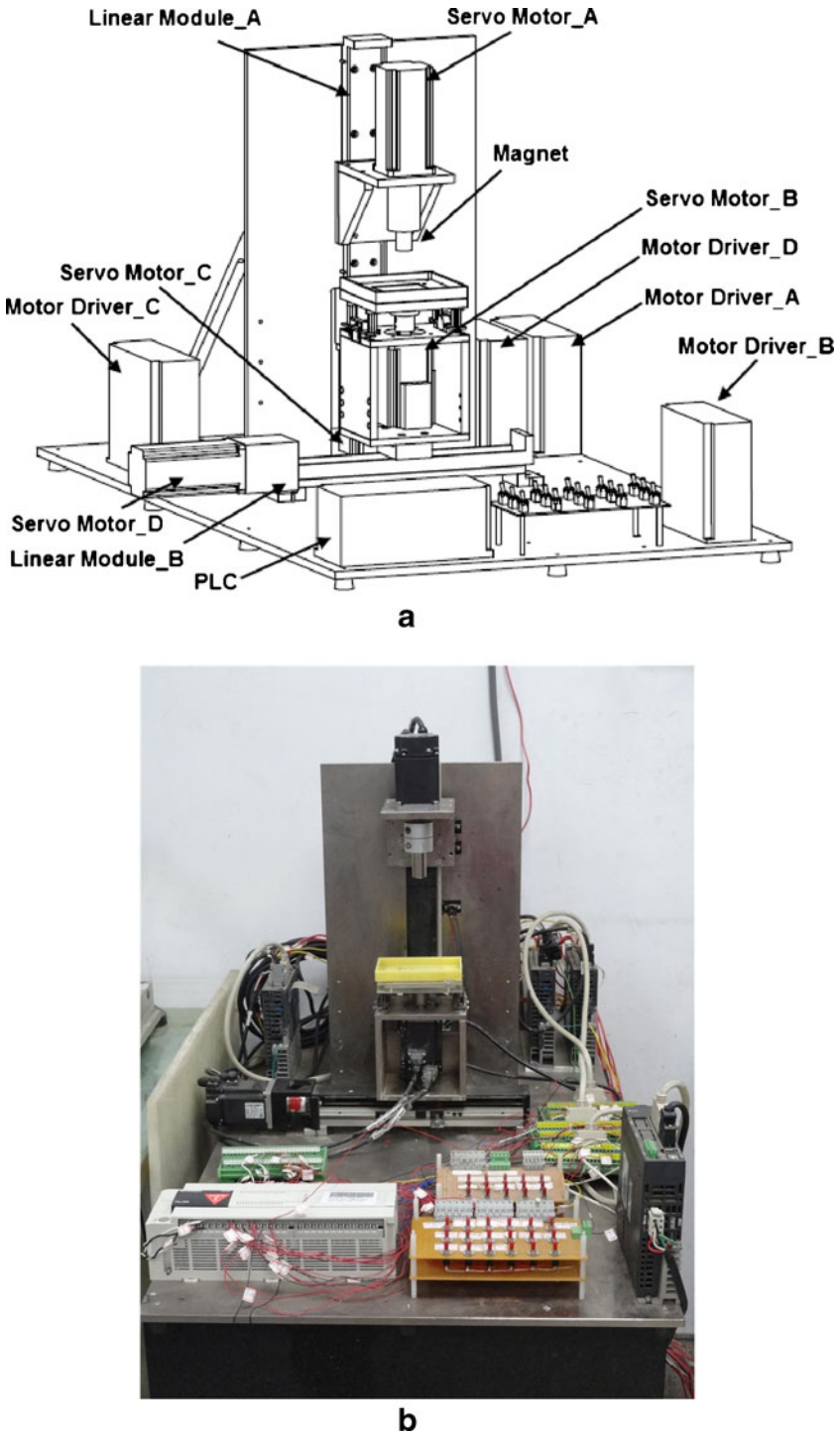

Fig. 1 **a** Schematic diagram and **b** actual photograph of 2D VAMAF platform

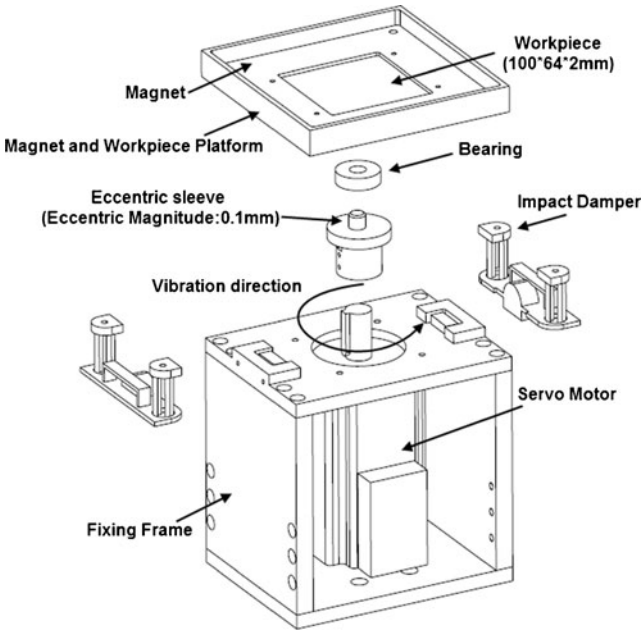

Fig. 2 Exploded view of vibration assistance mechanism

working gap and the slower the circumferential speed, the poorer the MRR is; and the faster the circumferential speed, the better the surface quality achieved. Hung et al. [11] used MAF to process cylindrical tube of stainless steel SUS304 and explored the processing characteristics and the prediction system. Their findings reveal that spindle speed, vibration frequency, discharge current, and abrasive weight ratio have significant influence on surface finish processed by MAF.

Polishing quality obtained by MAF under vibration assistance is closely related to the mode of vibration [12–14]. There are two modes of vibration. One mode is horizontal vibration on the *X*- or *Y*-axis of the workpiece, which serves to achieve self-sharpening or replacement of abrasive through back-and-forth motion along *X* or *Y* direction. Although horizontal vibration can enhance machining precision, there is still room for improvement with regard to reduction in machining time. The other mode is vertical vibration on the *Z*-axis of the workpiece, which serves to increase the opportunity of impact between the steel particles and SiC abrasives within the working gap of the workpiece and magnetic brush. Comparatively, horizontal vibration can achieve more efficient MRR and yield better surface quality than vertical vibration.

In view of the above, this study uses two-dimensional vibration-assisted MAF (2D VAMAF) to form dense intersecting machining paths under simultaneous vibration in both *X*- and *Y*-axes, which can help improve machining efficiency, enhance surface quality, and reduce machining time required. In addition, nonsintered magnetic abrasives comprising steel particles mixed with SiC abrasives are used under vibration to achieve better surface quality on the polished stainless steel. Experimental results show that 2D VAMAF is superior to MAF in rapid polishing of stainless steel workpiece with less scratching made on the finished surface.

2 Experimental design

2.1 Experimental setup

Figure 1 shows the schematic diagram and actual photograph of the self-developed 2D VAMAF platform. As can be seen, the 2D VMAF control system is composed of the programmable logic controller (PLC), motor drivers, and servo motors. Motor drivers receive digital signals sent by the PLC to drive the servo motors for different adjustments and controls so as to ensure that machining was conducted under the same conditions. Servo motor A is for adjusting the rotational speed of magnet (range, 100–1,000 rpm); servo motor B is for adjusting the rotational speed of eccentric sleeve so as to control the frequency of vibration of workpiece (range, 0–16.67 Hz), servo motor C is for adjusting the working gap (range, 0.5–2 mm), and servo motor D is for controlling the position of the workpiece.

2.2 Vibration assistance mechanism

Figure 2 shows the exploded view of the vibration assistance mechanism. As can be seen, the magnet and workpiece platform is connected by a bearing to the eccentric sleeve, which vibrates at 0.1-mm amplitude when driven by a servo motor. The magnet and workpiece platform is supported by two plastic impact dampers, one on each side. These dampers provide a cushioning effect to prevent rotation of workpiece under vibration along *X* and *Y* directions. The force distributions along the three axes during vibration-assisted polishing are measured using a load cell installed beneath the platform.

2.3 Materials and methods

The $100 \times 64 \times 2$ mm^3 workpiece is made of SUS 304 stainless steel. It is manufactured first by hot rolling, followed by cold rolling, and finally processed into a flat surface. Table 1 shows

Table 1 Chemical composition of SUS304stainless steel

Chemical composition (wt%)	C	Si	Mn	P	S	Ni	Cr
	≤0.08	≤1.0	≤2.0	≤0.035	≤0.03	8.0–10.5	18.0–20.0

Table 2 Experimental parameters and levels for 2D VAMAF

Factors	Level 1	Level 2	Level 3
Working gap (mm)	1	2	
Weight of SiC (g)	1	2	3
Weight of steel particles (g)	1	1.5	2
Weight of machining fluid (g)	1	2	3
Frequency of vibration (Hz)	0 (0 rpm)	8.33 (500 rpm)	16.67 (1,000 rpm)
Rotational speed of magnet (rpm)	100	500	1,000
Particle size of Sic	#1000 (18 μm)	#3000 (6 μm)	#8000 (1 μm)
Particle size of steel grit	#50 (0.3 mm)	#80 (0.18 mm)	#120 (0.125 mm)

the chemical composition of SUS 304 stainless steel. The SiC abrasives and the magnetic steel particles are first weighed with a high-precision electronic balance and then mixed together with the machining fluid SAE40. The machining tool of 20-mm diameter and 50-mm length is made of N35 Nd-Fe-B magnet.

Table 2 displays the experimental parameters and levels for 2D VAMAF. Prior to MAF, the SiC abrasives and the magnetic steel particles are weighed and then mixed together with the machining fluid SAE40. The workpiece is first washed in an ultrasonic cleaner for 20 min before being placed onto the 2D VAMAF platform for machining. After 5-min processing, the workpiece is again washed in an ultrasonic cleaner for 20 min. Its surface morphology is then examined under scanning electron microscope (SEM; Hitachi S3500N) and its surface roughness is determined using a surface roughness measurement instrument (Kosaka Laboratory SEF-3500). Figure 3 illustrates the area machined and the region observed. Four observations are made on each workpiece specimen with each observation made after rotating counterclockwise the workpiece specimen at 90°.

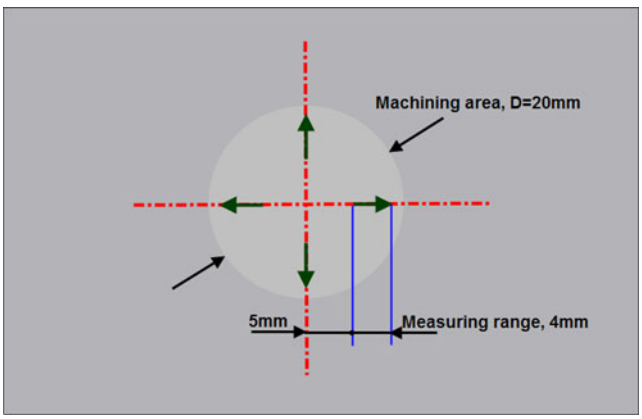

Fig. 3 Machined area and observed region on workpiece

3 Results and discussion

3.1 Effect of vibration assistance on MAF

Figure 4 illustrates the changes in surface roughness with processing time of MAF and 2D VAMAF. For the initial 50 s, measurement is taken every 10 s and thereafter at an interval of 60 s. As can be seen, surface roughness decreases with processing time with more marked decline within the first minute. In addition, regardless of the processing time, 2D VAMAF yields better surface roughness than MAF, and the difference in Ra value increases with processing time. MAF and 2D VAMAF reduced Ra from 0.13 to 0.06 μm and 0.03 μm, a decrease of 54 and 77 %, respectively. These results indicate that 5-min 2D VAMAF can improve surface roughness to 0.03 μm and vibration assistance does contribute to higher performance of MAF, resulting in better surface quality.

Figures 5 and 6 show SEM images and 3D surface profiles of workpiece surface before and after 5-min polishing with and without vibration assistance. Compared with the original

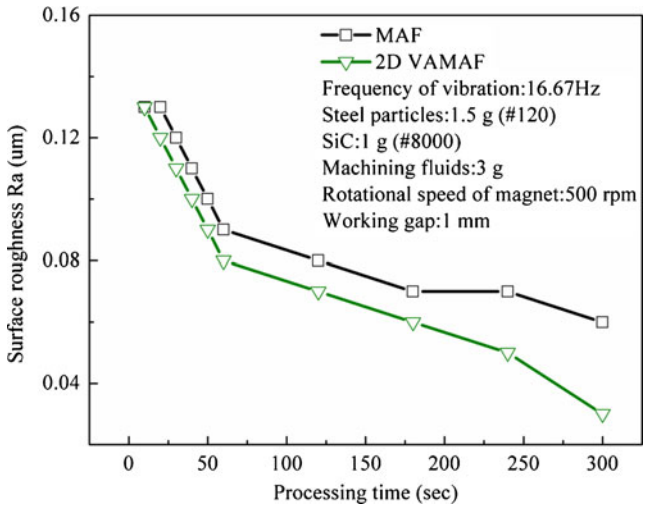

Fig. 4 Changes in surface roughness with processing time

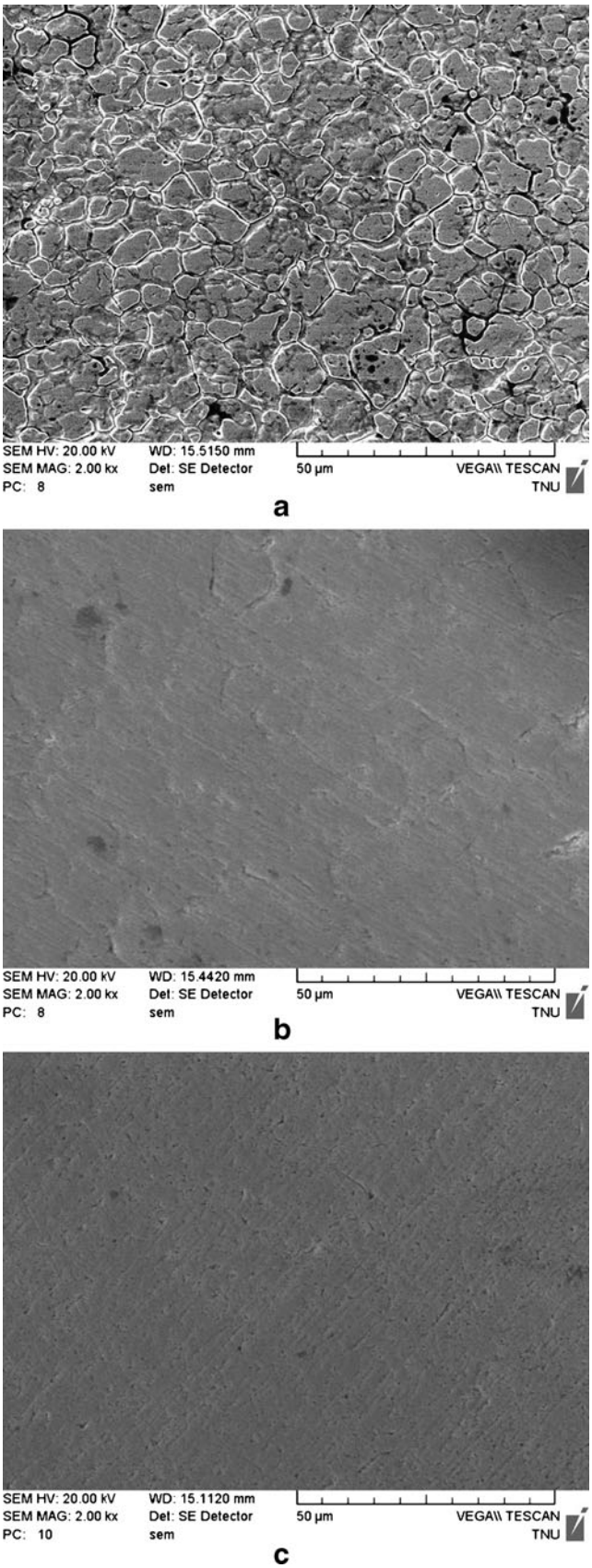

Fig. 5 SEM images of workpiece surface **a** before and after 5-min polishing by **b** MAF and **c** 2D VAMAF

workpiece surface (Ra=0.13 μm) seen in Fig. 5a, the surfaces polished by MAF (Ra=0.06 μm) and 2D VAMAF (Ra=0.03-μm), as seen in Figs. 5b,c, respectively, show much lower surface roughness. These images echo the results shown in Fig. 4 that MAF can indeed improve surface roughness and with vibration assistance, even better surface quality can be achieved. Similarly, the 3D surface profiles show great improvement in surface roughness of the polished workpiece (Figs. 6b,c) compared with the original (Fig. 6a). While scratches can still be found on the workpiece machined by MAF, much less surface roughness is observed for the workpiece polished by 5-min 2D VAMAF.

Figure 7 illustrates the force distributions along the three axes during vibration-assisted polishing from 0 to 140 s. As can be seen, there is an increase in force in all three directions in the first 20 s, during which the servo motor starts driving the rotation of magnet from vibration frequency 0 Hz to reach the required frequency. Upon reaching the required frequency, the acceleration stops and the force ceases to increase further but remains constant. Since this study aims to examine MAF under 2D vibration, no machining tool is installed on the *Z*-axis.

Moreover, the force is evenly distributed along the *X* (Fig. 7a), *Y* (Fig. 7b), and *Z* (Fig. 7c) axes with F_X=1.76 N, F_y=1.47 N, and F_z=0.63 N measured during 20–140 s. In other words, the force exerted on the workpiece along the *Z*-axis of the vibration-assisted platform is comparatively smaller. Not only are the forces along both *X*- and *Y*-axes larger, they are also steady and uniform.

3.2 Optimal parameter combination of 2D VAMAF

3.2.1 Taguchi's orthogonal experiment

Table 3 lists the combination of factors in the L18 ($2^1 \times 3^7$) orthogonal array established using the Taguchi experimental design method [15–19] and the surface roughness obtained for each parameter combination. All the experiments were conducted in triplicate for 5 min as per the conditions given in the table. Analysis of variance (ANOVA) was employed to assess the significant machining parameters affecting surface quality. The optimal combination of parameters derived from the Taguchi experimental design and ANOVA was subject to reproducibility analysis. Experimental findings were compared with the predicted results to validate the optimal combination of parameters.

Figure 8 shows the effect of different combinations of parameters on polishing performance denoted by the signal-to-noise (S/N) ratio. In this work, the predicted value of surface roughness should be "the lower the better" (LB). The S/N ratio, in unit of decibel, is calculated using the following equations:

$$LB : \eta = -10\log\left[\frac{1}{n}\sum_{i=1}^{n} yi^2\right] \quad (1)$$

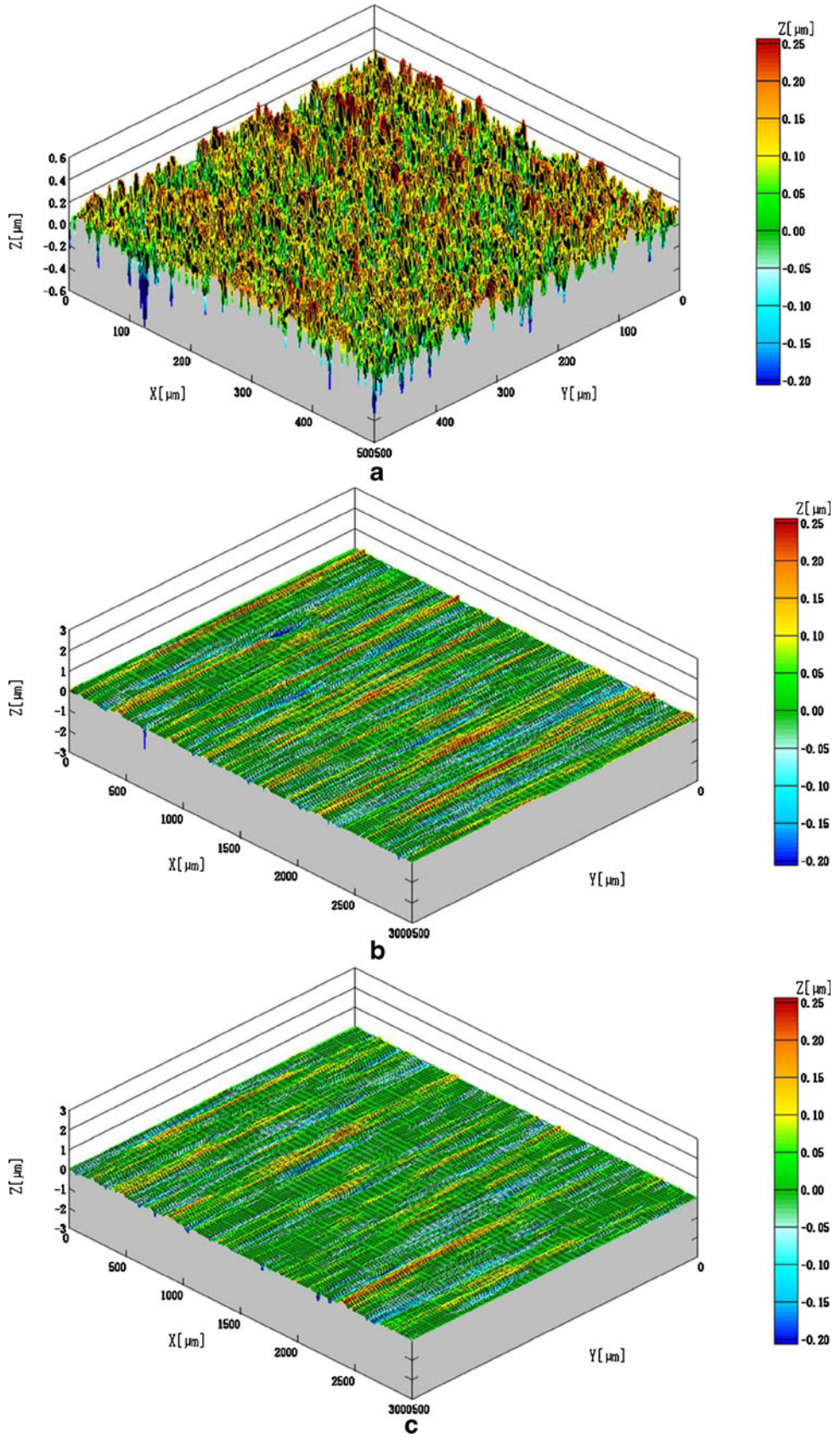

Fig. 6 3D surface profiles of workpiece surface **a** before and after 5-min polishing by **b** MAF and **c** 2D VAMAF

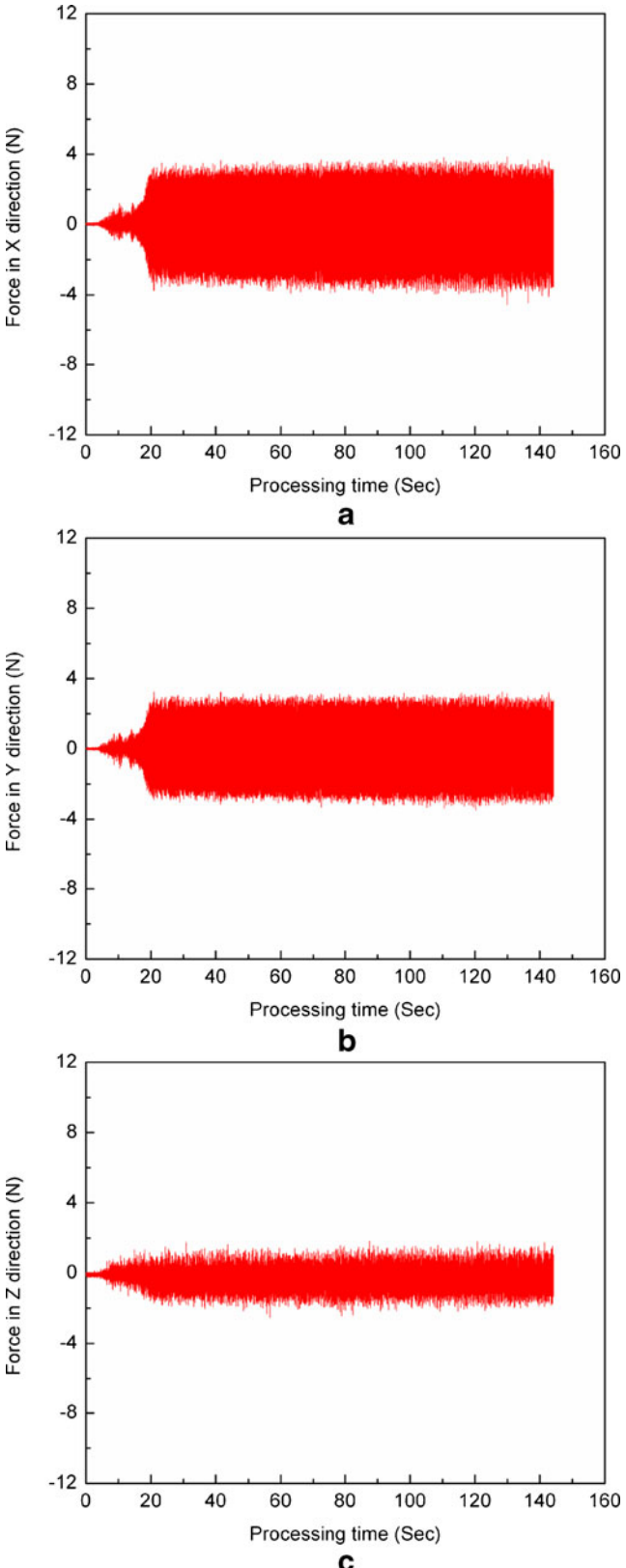

Fig. 7 Force distribution of workpiece in **a** *X*-, **b** *Y*-, and **c** *Z*-direction during vibration-assisted polishing

where *yi* denotes the experimental values of the *i*th experiment and *n* denotes the number of experiments performed.

$$\left[\frac{S}{N}\right]_{predicted} = \left[\frac{S}{N}\right]_m + \sum_{i=1}^{n}\left(\left[\frac{S}{N}\right]_i - \left[\frac{S}{N}\right]_m\right) \quad (2)$$

where $[S/N]_{predicted}$ is the predicted S/N ratio, $[S/N]_m$ is the mean of all 18 S/N ratios obtained, and $[S/N]_i$ is the S/N ratio of the *i*th experiment. The predicted surface roughness obtained using the optimal combination of parameters can be calculated using Eqs. (1) and (2).

According to the results shown in Fig. 8, the optimal combination of parameters should be A1B1C2D3E3F2G3H3; that is, working gap (1 mm);weight of SiC, steel particles, and machining fluid (1, 1.5, and 3 g, respectively); frequency of vibration (16.67 Hz); rotational speed of magnet (500 rpm); and particles size of SiC and steel particles (#8000 and #120), respectively.

3.2.2 ANOVA and F test results

Table 4 lists the ANOVA results of surface roughness. The parameters in order of their contribution percentage are particle size of SiC>working gap>frequency of vibration>weight of SiC>weight of machining fluid. In all types of machining and polishing, the particle size of the abrasive, SiC in this study, has

Table 3 Design of experimental matrix and results

EXP	Factors								Surface Roughness	
	A	B	C	D	E	F	G	H	Ra (μ m)	S/N Ratio (dB)
1	1	1	1	1	0	100	1,000	50	0.105	19.576
2	1	1	1.5	2	8.33	500	3,000	80	0.070	23.098
3	1	1	2	3	16.67	1,000	1,000	50	0.030	30.457
4	1	2	1	1	8.33	500	8,000	120	0.115	18.786
5	1	2	1.5	2	16.67	1,000	1,000	50	0.055	25.192
6	1	2	2	3	0	100	3,000	80	0.080	21.938
7	1	3	1	2	0	1,000	3,000	120	0.065	23.741
8	1	3	1.5	3	8.33	100	800	50	0.090	20.915
9	1	3	2	1	16.67	500	1,000	80	0.075	22.498
10	2	1	1	3	16.67	500	3,000	50	0.085	21.411
11	2	1	1.5	1	0	1,000	8,000	80	0.055	25.192
12	2	1	2	2	8.33	100	1,000	120	0.125	18.061
13	2	2	1	2	16.67	100	8,000	80	0.115	18.786
14	2	2	1.5	3	0	500	1,000	120	0.105	19.576
15	2	2	2	1	8.33	1,000	3,000	50	0.115	19.576
16	2	3	1	3	8.33	1,000	1,000	80	0.075	22.498
17	2	3	1.5	1	16.67	100	3,000	120	0.100	20.000
18	2	3	3	2	0	500	8,000	50	0.105	19.576

A Working gap (in millimeter), *B* Weight of SiC (in gram), *C* weight of steel particles (in gram), *D* weight of machining fluid (in gram), *E* frequency of vibration (in Hertz), *F* rotational speed of magnet (in rotations per minute), *G* particle size of Sic, *H* particle size of steel grit

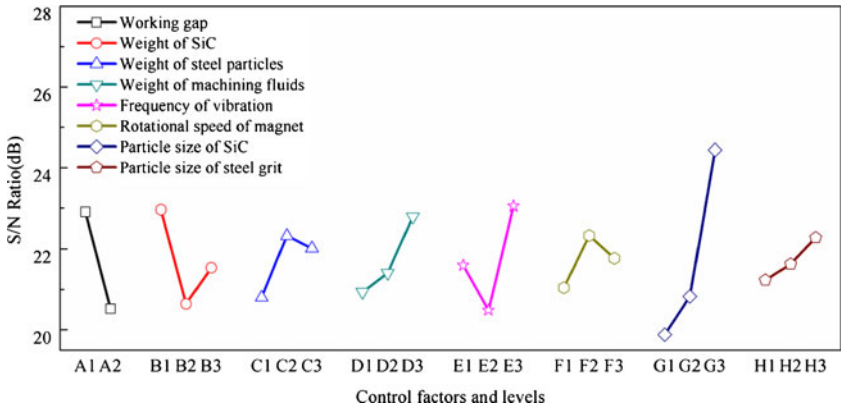

Fig. 8 Effect of polishing parameters on surface quality

direct influence on the size of scratch marks left on the finished surface. Similarly, the working gap is the chief determinant of the magnetic force for machining. Hence, these two parameters play key roles in 2D VAMAF. Frequency of vibration along *X* and *Y* directions, which is the main focus of this study, also has significant impact on the final surface quality.

3.2.3 Confirmation experiment

Reproducibility analysis was then performed to verify the optimal parameter values derived from the Taguchi method and ANOVA. Table 5 compares the calculated and experimental results obtained by the optimal parameter combination. As can be seen, in all three trials, the same results are obtained with the calculated values close to the actual surface roughness measured, indicating reliability of the Taguchi design method.

Table 4 ANOVA and *F* test results

Factors	DOF	Sum of squares	Mean square	*F* value	Contribution (%)
A	1	25.740	25.740	5.388*	16.048
B	2	16.483	8.241	1.725	10.276
C	(2)	7.837			
D	2	11.238	5.619	1.176	7.006
E	2	19.911	9.956	2.084	12.414
F	(2)	5.051			
G	2	69.633	34.816	7.288**	43.413
H	(2)	3.387			
A×B	(2)	1.116			
Error	6	9.554	8.696		10.843
Total	17	160.395			100.000

A Working gap (in millimeter), *B* Weight of SiC (in gram), *C* weight of steel particles (in gram), *D* weight of machining fluid (in gram), *E* frequency of vibration (in Hertz), *F* rotational speed of magnet (in rotations per minute), *G* particle size of Sic, *H* particle size of steel grit

Figure 9 displays the surface quality achieved by 5-min 2D VAMAF using the optimal parameter combination. As can be seen, the polished stainless steel surface with surface roughness of only 0.03 μm show mirror reflection.

3.3 Effect of significant machining parameters on surface roughness

3.3.1 Effect of SiC particle size on surface roughness

Figure 10 shows the changes in surface roughness with SiC particle size under different frequencies of vibration. As can be seen, surface roughness decreases with reduction in SiC particle size. Moreover, the smaller the SiC particle size, the greater the improvement in surface roughness is. Upon contact with the workpiece, large particles tend to leave deeper scratches on the workpiece surface. Hence, better polishing effect is achieved by particles of smaller size. In addition, the higher the vibration frequency, the smaller the surface roughness is. With the same polishing time, higher frequency of vibration results in more frequent contact of the abrasives with the workpiece. Consequently, better polishing performance can be achieved which yields enhanced surface quality.

3.3.2 Effect of working gap on surface roughness

Figure 11 displays the changes in surface roughness and magnetic flux density with working gap. As can be seen, the

Table 5 Calculated and experimental results of optimal parameter combination

Trial no.	Surface roughness Ra (μm)	
	Calculated	Experimental
1	0.028	0.03
2	0.028	0.03
3	0.028	0.03

Fig. 9 Surface with mirror reflection achieved by 2D-VAMAF

lowest surface roughness of 0.03 μm is obtained at 1-mm working gap with magnetic flux density of 0.27 T. When the working gap is increased to 2 mm, surface roughness becomes worse, rising to 0.07 μm with magnetic flux density of 0.21 T. As known, there exists an inverse relationship between working gap and magnetic flux density. Hence, a decrease in working gap would lead to an increase in magnetic flux density, which would in turn cause cramming of abrasives on the workpiece surface. As a result, surface quality deteriorates. However, an increase in working gap would lead to a decrease in magnetic flux density, which would also reduce the normal force of the abrasives on the workpiece, thus undermining the polishing efficiency. Hence, the optimal working gap as observed in Fig. 11 should be 1 mm for achieving the best surface quality.

3.3.3 Effect of vibration frequency on surface roughness

Figure 12 shows the changes in surface roughness with different frequencies of vibration under different rotational speeds of magnet. As can be seen, surface roughness decreases with increasing frequency of vibration. In other words,

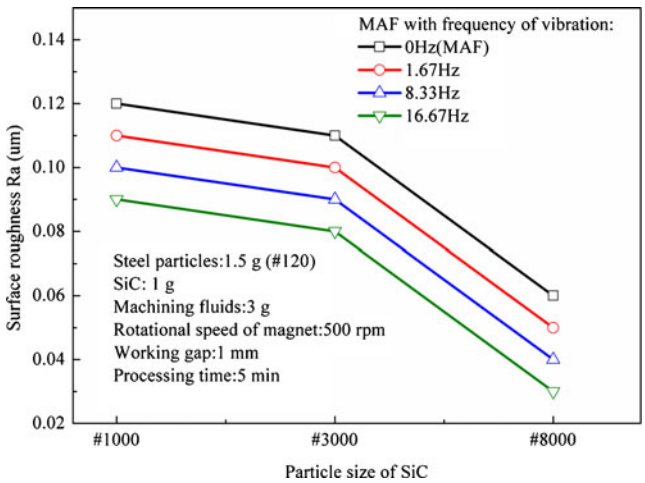

Fig. 10 Changes in surface roughness with SiC particle size

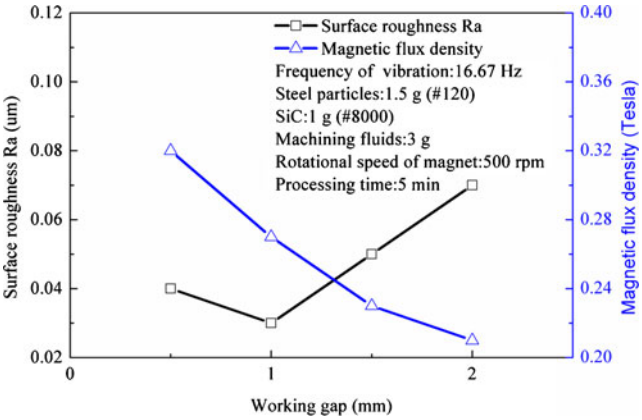

Fig. 11 Changes in surface roughness and magnetic flux density with working gap

the efficiency of MAF can be enhanced under vibration assistance, which echoes the findings of better polishing performance and better surface roughness obtained by 2D VAMAF mentioned above. Moreover, further increase in vibration frequency leads to even lower surface roughness. With 5-min machining on a workpiece with vibration frequency of 16.67 Hz, a good-quality surface with roughness of 0.03 μm can be obtained. However, the rotational speed of magnet does not follow the same trend as the frequency of vibration. While it is true that better surface roughness is obtained with increasing rotational speed of magnet, the reverse is true with rotational speed above 500 rpm. At low rotational speed of magnet, the relative motion between abrasives and workpiece is kept so low that there is limited abrasion. However, a too-high rotational speed of the magnet will foster the dispersion of abrasives from the working gap, which would in turn deteriorate polishing performance.

3.3.4 Effect of SiC weight on surface roughness

Figure 13 shows the changes in surface roughness with weight of SiC under MAF and 2D VAMAF. As can be seen, lower

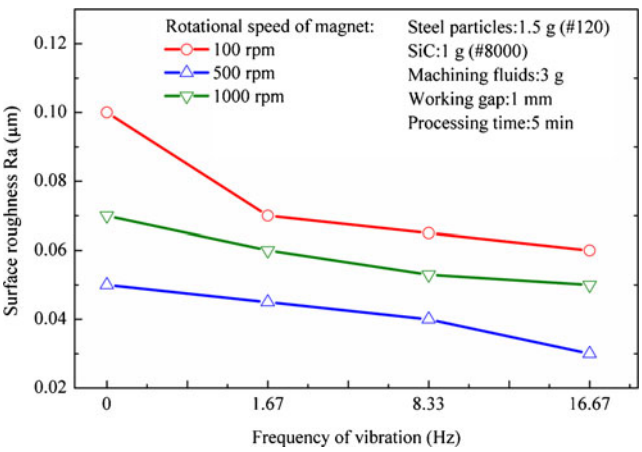

Fig. 12 Changes in surface roughness with frequency of vibration

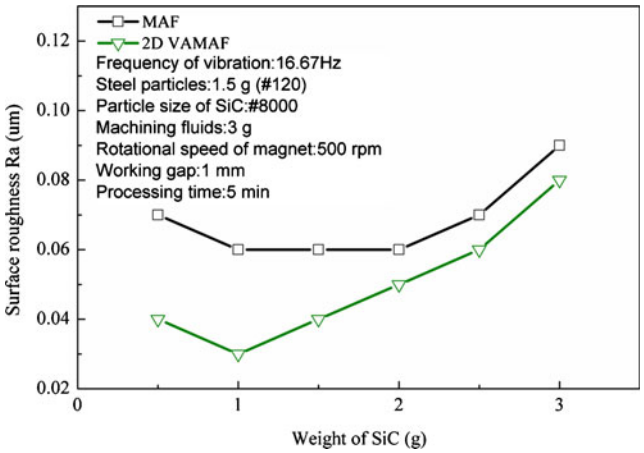

Fig. 13 Changes in surface roughness with SiC weight

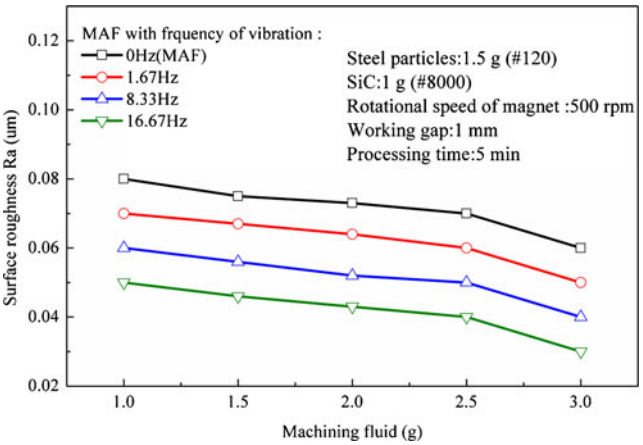

Fig. 14 Changes in surface roughness with machining fluid weight

surface roughness is obtained under vibration assistance. At vibration frequency of 16.67 Hz, the lowest surface roughness of 0.03 μm is obtained for SiC weight of 1 g. Further increase in weight of SiC yields higher surface roughness. At SiC weight of 3 g, the surface roughness for MAF with and without vibration assistance increases to 0.08 μm. The optimal ratio of SiC to machining fluid added is 1:3. A too-low mixing ratio will result in a thin diluted mixture not ideal for machining while a too-high mixing ratio will yield a thick mixture that impedes the self-sharpening of abrasives. Hence, for the same amount of machining fluid used, adding too little or too much SiC would affect polishing performance. The main difference between 2D VAMAF and MAF is the vibration added, which not only contributes to self-sharpening of the abrasives but also enhances the relative motion between abrasives and workpiece. Hence, under vibration assistance, 2D VAMAF shows comparatively better polishing performance and yields better surface roughness with a shorter machining time and a smaller amount of abrasives required.

3.3.5 Effect of machining fluid weight on surface roughness

Figure 14 shows the changes in surface roughness with weight of machining fluid under different frequencies of vibration. As can be seen, there exists an inverse relationship between the two. In other words, with sufficient SiC added, the higher the weight of machining fluid, the lower the surface roughness obtained. Greater amount of machining fluid used can enhance the replacement of abrasives and increase the rate of debris removal, thus contributing to better polishing efficiency. In addition, the curves also reveal that lower surface roughness is achieved with vibration; and the higher the vibration frequency, the better the surface quality obtained. Such findings are consistent with what has been mentioned above.

4 Conclusions

This study explores the effects of adding vibration to conventional MAF for enhancing polishing performance and improving surface quality. The following conclusions are drawn from the experimental results.

1. 2D VAMAF can effectively increase the polishing efficiency of MAF and improve surface quality. In addition to MAF by steel particles and SiC abrasives, dense intersecting machining paths on the workpiece are also formed under vibration assistance, thus contributing to better polishing efficiency and precision.
2. Obtained by the Taguchi experimental design, the optimal combination of parameters for improving surface roughness includes working gap (1 mm); weight of SiC, steel particles, and machining fluid (1, 1.5, and 3 g, respectively); frequency of vibration along *X*- and *Y*-directions (16.67 Hz); rotational speed of magnet (500 rpm); and size of SiC and steel particles (#8000 and #120), respectively.
3. With 5-min 2D VAMAF under optimal parameter combination, the surface roughness of a stainless steel SUS304 workpiece can be reduced from 0.13 to 0.03 μm, an improvement of 77 %.
4. 3D profiles of finished surface evidence the efficient removal of scratches under MAF and further enhancement in surface quality can be obtained under vibration assistance.

References

1. Jain VK, Kumar P, Behera PK, Jayswal SC (2001) Effect of working gap and circumferential speed on the performance of magnetic abrasive finishing process. Wear 250:384–390
2. Mulik RS, Pandey PM (2011) Magnetic abrasive finishing of hardened AISI 52100 steel. Int J Adv Manuf Technol 55(5–8):501–515
3. Amineh SK, Tehrani AF, Mohammadi M (2013) Improving the surface quality in wire electrical discharge machined specimens by removing the recast layer using magnetic abrasive finishing method. Int J Adv Manuf Technol 66(9–12):1793–1803
4. Givi M, Tehrani AF, Mohammadi A (2012) Polishing of the aluminum sheets with magnetic abrasive finishing method. Int J Adv Manuf Technol 61(9–12):989–998
5. Liu ZQ, Chen Y, Li YJ, Zhang X (2013) Comprehensive performance evaluation of the magnetic abrasive particles. Int J Adv Manuf Technol. doi:10.1007/s00170-013-4783-6
6. Mulik RS, Pandey PM (2010) Mechanism of surface finish in ultrasonic-assisted magnetic abrasive finishing process. Mater Manuf Process 25:1418–1427
7. Mulik RS, Pandey PM (2011) Ultrasonic assisted magnetic abrasive finishing of hardened AISI 52100 steel using unbonded SiC abrasives. Int J Refract Met Hard Mater 29:68–77
8. Yin S, Shinmura T (2004) Vertical vibration-assisted magnetic abrasive finishing and deburring for magnesium alloy. Int J Mach Tool Manuf 44:1297–1303
9. Wang Y, Hu D (2005) Study on the inner surface finishing of tubing by magnetic abrasive finishing. Int J Mach Tool Manuf 145:43–49
10. Wang D, Shinmura T, Yamaguchi H (2004) Study of magnetic field assisted mechanochemical polishing process for inner surface of Si_3N_4 ceramic components: finishing characteristics under wet finishing using distilled water. Int J Mach Tool Manuf 44:1547–1553
11. Hung CL, Ku WL, Yang LD (2010) Prediction system of magnetic abrasive finishing (MAF) on the internal surface of cylindrical tube. Mater Manuf Process 25:1404–1412
12. Shinmura T, Takazawa K, Hatano E (1986) Study on magnetic abrasive finishing (1st report): process principle and a few finishing characteristics. J Jpn Soc Precis Eng 52:851–857
13. Shinmura T, Hatano E, Takazawa K (1986) Development of plane magnetic abrasive finishing apparatus and its finishing performance. J Jpn Soc Precis Eng 52:1080–1086
14. Kim JD, Choi MS (1997) Study on magnetic of polishing free-form surface. Int J Mach Tool Manufact 37:1179–1187
15. Singh S, Shan HS, Kumar P (2002) Parametric optimization of magnetic-field-assisted abrasive flow machining by the Taguchi method. Qual Reliab Eng Int 18:273–283
16. Liao HT, Shie JR, Yang YK (2008) Applications of Taguchi and design of experiments methods in optimization of chemical mechanical polishing process parameters. Int J Adv Manuf Technol 38:674–682
17. Yang LD, Lin CT, Chow HM (2009) Optimization in MAF operations using Taguchi parameter design for AISI304 stainless steel. Int J Adv Manuf Technol 42(5–6):595–605
18. Mali HS, Manna A (2012) Simulation of surface generated during abrasive flow finishing of Al/SiCp-MMC using neural networks. Int J Adv Manuf Technol 61:1263–1268
19. Prabhu S, Vinayagam B (2012) AFM investigation in grinding process with nanofluids using Taguchi analysis. Int J Adv Manuf Technol 60:149–160